Polymer Bulletin (2023) 80:2171–2185
https://doi.org/10.1007/s00289-022-04549-9

ORIGINAL PAPER

Doxorubicin and tamoxifen loaded graphene oxide nanoparticle functionalized with chitosan and folic acid for anticancer drug delivery

Nese Keklikcioglu Cakmak[1] · **Atakan Eroglu**[1]

Received: 4 July 2022 / Revised: 23 September 2022 / Accepted: 24 October 2022 /
Published online: 12 November 2022

Abstract

Research has commonly utilized graphene-based drug delivery systems for a long time to achieve effective cancer treatment. In the present study, doxorubicin (DOX) and selective estrogen receptor modulator tamoxifen (TAM) anticancer drugs used in breast cancer treatment were bound to a graphene oxide (GO)-based and folic acid (FA)-targeted nanocarrier system that was made biocompatible with chitosan (CS). To this end, graphene oxide synthesis was primarily carried out by employing the modified Hummer's method, and then FA and CS were loaded on GO to obtain a targeted and biocompatible carrier The characterization of the obtained conjugate was performed by X-ray diffraction analysis, Fourier transform infrared spectroscopy, UV-visible spectrophotometry, scanning electron microscopy, and zeta potential analysis. The zeta potential values of all samples were checked and all of them have a zeta potential above the stability value of ± 25 mV. GO-CS-FA has the highest zeta potential of 68.8 mV. The graphene oxide-chitosan-folic acid-tamoxifen-doxorubicin (GO-CS-FA-TAM-DOX) nanocarrier-based drug displayed a pH-dependent drug release. The drug release profile from these systems was researched in two pH buffer solutions prepared as acidic (pH 5.8) and physiological (pH 7.4). The characterization analyses showed that the drugs bound successfully to the targeted delivery system. The drug release analyses demonstrated that GO-CS-FA-TAM-DOX was released better in the acidic (pH 5.8) medium compared to the physiological (pH 7.4) medium after 24 h.

Keywords Doxorubicin · Tamoxifen · Folic acid · Chitosan · Graphene oxide · Stability · Zeta potential

✉ Nese Keklikcioglu Cakmak
nkeklikcioglu@cumhuriyet.edu.tr

[1] Department of Chemical Engineering, Faculty of Engineering, Sivas Cumhuriyet University, 58140 Sivas, Türkiye

Introduction

Cancer represents a serious disease that threatens life and causes abnormal cell growth with the possibility of invading the body's other parts. Lung, liver, bladder, colon and rectal, breast, sarcoma, kidney, endometrial, leukemia, melanoma, head and neck, pancreatic, cervix, prostate, etc. are among the frequently diagnosed types of cancer around the world [1]. Breast cancer is in the second place among the most frequently diagnosed female cancers, and only lung cancer exceeds it [2]. Nowadays, surgery, chemotherapy, radiotherapy, hormone therapy, immunotherapy, laser therapy, therapeutic drugs or stem cell transplants are used in cancer treatment. The objective of all treatments is the complete removal or destruction of cancerous tissues without damaging healthy tissues. However, cancer remains the primary cause of death among people, and novel therapeutic strategies must be designed for cancer therapy.

Doxorubicin (DOX) and tamoxifen (TAM) are chemotherapeutic drugs frequently used in breast cancer treatment. DOX is among the agents with the highest efficiency available for treating metastatic breast cancer. DOX is an anticancer anthracycline antibiotic and frequently utilized to treat many cancers such as bladder, breast, ovarian, lung, and gastric cancer [3–7]. DOX is involved in various molecular mechanisms at the cellular level, such as the intercalation of the two nitric bases of the DNA double helix, the formation of free radicals causing DNA damage, the inhibition of respiratory chain enzymes in mitochondria, and the oxidation of membrane lipids. Although DOX has a high chemotherapeutic potential, it also has serious dose-related side effects such as cardiomyopathy, heart failure, and the development of drug resistance. Additionally, DOX is degraded quickly and eliminated following intravenous administration [8]. Hence, numerous attempts have been exerted to produce new DOX analogs and reformulate the DOX molecule. It remains the focus of clinical trials to identify new strategies for more effective use of DOX in cancer therapy [9–11].

Selective estrogen receptor modulators (SERMs), e.g., lasofoxifene, bazedoxifene, tamoxifen, and raloxifene, are challenged at the moment for treating breast cancer, osteoporosis, and postmenopausal symptoms since they can perform functions of estrogen receptors agonist or antagonist, according to the target tissue [12, 13]. TAM is a non-steroidal anti-estrogen. The U.S. Food and Drug Administration (FDA) approved it for the first time for metastatic breast cancer treatment in 1977. The mentioned chemotherapeutic agent is also commonly utilized for the purpose of reducing the recurrence of primary breast cancer and contributes to survival rates as adjuvant therapy [14, 15]. TAM represents an antitumor drug that has been used around the world for over 30 years in treating estrogen receptor (ER)-positive metastatic and adjuvant breast cancer [13]. Because of the low solubility of TAM and its metabolites in aqueous solutions, the administration of such anticancer drugs creates a considerable difficulty in breast cancer therapeutics. Low solubility and selectivity are the most frequent disadvantages of TAM. Hence, the long-term use of the drug increases the risk of uterine cancer [16–18].

In recent times, nanotechnology has been regarded as a crucial technology in the pharmaceutical area and has drawn significant attention in the area of nanomedicine [19–21]. Nanomedicine is among the nanotechnology applications with the highest potential in the medical field and is considered a crucial strategy to diagnose and treat cancer [22]. More rapid drug diffusion in the body and directing them to the specific target are ensured by nanoparticle application [20–23].

Chemotherapeutic drugs that are available at the moment are agents with low molecular weight and high cytotoxicity and pharmacokinetic volume of distribution. Ultimately higher concentration is required in order to facilitate the excretion of these low molecular weight drugs, causing higher toxicity and undesirable side impacts such as consequent hair loss and bone marrow suppression. The drugs in question have no tissue specificity and lead to serious damage to normal non-cancerous cells [24]. With the objective of overcoming the mentioned disadvantages, many nanocarrier systems, such as silica nanoparticles, polymer nanoparticles, microspheres, liposomes, and inorganic materials, have been developed as anticancer drug carriers. Owing to these nanocarrier systems, drugs can be transported directly to target cancer cells by binding with target molecules and released under appropriate controlled conditions [25, 26].

Using nanocarrier systems is a promising strategy for making DOX and TAM more controlled and targeted drugs [11, 27, 28]. These nanocarrier systems allow drugs to evade the body's biological attacks and reach the tumor site in a higher concentration with increased permeability and retention impact in passive targeting and reverse MDR [29, 30]. Furthermore, these nanocarrier systems can target the tumor in a selective way via bindings between targeting moieties loaded on the surface of nanoparticles and receptors specific to each cancer type [31].

At present, carbon-based nanomaterials are extensively utilized in applications in biomedicine, e.g., radiotherapy, drug delivery, photodynamic therapy, photothermal therapy, and diagnostic imaging [32–34]. Graphene, one of the carbon-based nanomaterials, and its derivative have caused the increased usage of carbon-based compounds in biomedicine due to its original structure and features. Concerning the chemical features of graphene and its derivatives, the presence of functional groups, e.g., hydroxyls (OH), carboxylic acid (COOH), and epoxides (COC), on its surface, particularly in graphene oxide (GO) and reduced graphene oxide (rGO), ensures graphene coupling to various biomolecules, making its applications in biomedicine more diverse [35–38]. It has been confirmed that graphene-based nanomaterials represent a possible platform for the treatment of cancer. GO has a two-dimensional (2D) crystalline structure comprised of carbon and has a hexagonal pattern with a few functional oxygen groups on its surface. GO is regarded as a more powerful tempering element with high biodetection potential due to π–π and/or n–π orbital interactions, sp^2 hybridization, and its variable bioconjugation chemicals [39]. It is easy to combine the functional groups of GO with other biomaterials and biomolecules. Moreover, easy dissolution in water and other solvents because of the functional oxygen groups constitutes GO's advantage [40, 41]. Graphene oxide is conjugated with different polymers to increase drugs' solubility, prevent blood cell aggregation, and enhance the drug's bioavailability and biocompatibility [42, 43]. In the current study, CS was used as a natural biopolymer to acquire a non-toxic, biodegradable and biocompatible nanocomposite obtained by

chitin deacetylation [44–47]. Additionally, due to the overexpression of folate receptors on cancer cells, FA was used within the scope of the study to conjugate the drug carrier with folic acid in order to make it a targeted carrier [48]. Carrier surfaces are conjugated with hydrophilic polymers or targeting ligands with the objective of improving systemic biocompatibility and increasing tumor targetability. Considering the known overexpression of FA receptors in a number of cancerous cells, FA is regarded as a targeting agent [49].

Recent research has indicated that the existence of specific biomarkers on nanocarriers' surface will increase the activity of targeting [50, 51]. The said findings are consistent with those obtained by Deb, who concentrated on obtaining the targeted delivery of drugs by means of CPT. Furthermore, PEG-functionalized GO nanoparticles were decorated with FA and utilized to achieve the increased specificity and efficiency of drug uptake by cancer cells [52]. Graphene oxide-loaded Ce6 that was conjugated with folic acid (FA) was revealed to be a powerful candidate for active drug delivery in photodynamic therapy (PDT) [53]. The non-immunogenic, nontoxic, and stable characteristics of folic acid make it appropriate for conjugation with nanocomposites [54]. It has been stated that folic acid conjugated with nanographene oxide and polyvinylpyrrolidone (PVP) is a nanocomposite with high success in chemo-photothermal therapy [53].

In this research, we concentrate on reaching targeted drug delivery by utilizing doxorubicin and selective estrogen receptor modulators (SERMs), tamoxifen as a model drug. The different mechanism of action of the said drugs makes them candidates with high potential to generate a synergistic impact against breast cancer. With the aim of obtaining the increased specificity and efficiency of drug uptake by cancer cells, graphene oxide nanoparticles functionalized with chitosan were decorated with folic acid and utilized as a drug delivery system. The synthesis and characterization of the TAM and DOX-loaded drug delivery system were conducted by XRD, UV, SEM, FTIR, and zeta potential analysis. The drug loading and release profile from these systems was investigated.

Experimental

Materials and methods

Graphite flakes (< 20 µm, 12.01 g/mol), H_2SO_4 (98%), H_2O_2 (30%), DOX, TAM, ethanol, N (3-dimethylaminopropyl N ethylcarbodiimide) hydrochloride (EDC), folic acid, N Hydroxysuccinimide (NHS), acetic acid, and chitosan (CS) were procured from Sigma-Aldrich Co. HCl (37%) and KMnO4 were acquired from Merck and Tekkim Co, respectively.

Synthesis of chitosan-folic acid-functionalized graphene oxide nanobiocomposite

The fusion of graphene oxide-mediated nanobiocomposite functionalized with chitosan and folic acid was initiated with synthesizing graphene oxide (GO) nanoparticles by employing the modified Hummers' method**.** In the present work, GO was

synthesized by the improved Hummers' method suggested by Marcona et al. [55]. In the method in question, first, a homogeneous solution was obtained by blending H_2SO_4 (360 mL) and H_3PO_4 (40 mL). Then, 3 g of graphite powder was added to the solution, and its stirring at 80 °C was carried out in a magnetic stirrer for 6 h. Afterward, the mixture was cooled to room temperature and washed with purified water for the purpose of removing the acid residues. The resulting semi-oxidized graphite was added to 250 mL of H_2SO_4 at 0 °C for complete oxidation. Then, the gradual adding of 18 g of $KMnO_4$ was carried out, keeping the temperature below 20 °C, and the mixture stirring was performed at a temperature of 35 °C for a period of 4 h. Afterward, 2 L of distilled water was added to the solution. Then 40 mL of 30% H_2O_2 aqueous solution was added, and the color of the mixture turned bright yellow with air bubbles. With the aim of removing metal impurities in the mixture, 0.1 M HCl solution was utilized for the mixture purification 4 times, and the centrifugation of the final mixture with deionized water was performed a few times, and the resulting product was dried at 60 °C. Therefore, GO was turned into nanographene oxide as a result of ultrasonication.

Adding chitosan (1 wt%) to the acetic acid solution (10%) was carried out, and it was stirred for a night with the objective of acquiring a viscous chitosan solution. Afterward, 0.5% of GO solution (20 ml) was added to the chitosan solution, sonicated for a period of 45 min and stirred for a night [56]. The addition of NHS and EDC to the GO-CS solution (1 mg/ml) was performed, and they were sonicated for a period of 2 h. In order to achieve a receptor-specific target for cancerous cells, which conjugates by reacting with COOH groups, folic acid (0.5%) was added to the chitosan-conjugated GO to obtain graphene oxide-chitosan-folic acid nanobiocomposite (GO-CS-FA). Afterward, removing unbound materials was performed by dialysis against sodium bicarbonate solution for a period of 24 h [57].

Characterization

Morphological measurements and size characterization were performed with a scanning electron microscope (SEM) (TESCAN MIRA3 XMU FEG (Brno, Czechia)), 10 kV accelerating voltage and a 10 mm working distance. The powders were poured on a double-sided carbon tape on an aluminum stub, and the residue was cleaned by an air gun. To produce a conductive surface, 5 nm of gold was coated by a Quorum Q150R ES magnetron sputter (Birmingham, UK). The recording of the samples' Fourier transform infrared (FTIR) spectra was conducted in the range varying between 400 and 4000 cm^{-1}. X-ray diffraction (XRD) represents a significant characterization method, providing important data about materials' chemical composition and crystallographic structure. The powders were weighed and different compositions of the samples were prepared by mixing and homogenizing in an agate mortar. The crystal structure of the mixed powders were analyzed with Rigaku-Miniflex 600 with 1.54–1.56 Angstrom, Cu-Kα radiation, a per step counting time of 0.5 s and a step-width of 0.002 degree/min. To ensure that the samples are dispersed homogeneously, a UV–Vis spectrophotometer (UV-1280, Shimadzu, Japan) recorded the spectra of the samples prepared in the range of 200–800 nm.

The samples' zeta potentials were measured with a Malvern Zetasizer Nano *Z* zeta potential analyzer.

Drug loading and in-vitro controlled release

The anticancer drugs tamoxifen (2 mg) and doxorubicin (4 mg) were added to dimethyl sulfoxide (DMSO) as 1 ml each, and after stirring for a while in a magnetic stirrer, DOX-DMSO (4 mg/ml) and TAM-DMSO (2 mg/ml) were added dropwise into 20 ml GO-CS-FA solution and mixed for 30 min. After stirring, pH was adjusted to 8, and the mixture was stirred in a magnetic stirrer for 24 h. Repeated washing ensured the removal of the unbound drug, which was kept at 4 °C. They were diluted and calibrated at pH 7.4 in phosphate buffer saline (PBS). The loading efficiency was computed in the following way:

$$\text{Loading efficiency (LE)} = (\text{total amount of drug} - \text{unbound drug})/\text{total amount of drug} \times 100\%$$

To prepare 500 ml PBS solution, NaCl (4 g), KCl (100 mg), Na_2HPO_4 (720 mg), and KH_2PO_4 (120 mg) were added into 400 ml distilled water, respectively, and another 100 ml distilled water was added to make up to 500 ml. The release rate of DOX and TAM-loaded GO-CS-FA was determined as a result of the dialysis of the sample against 50 ml of PBS at a temperature of 37 °C and pH of 5.8 (endosomal pH of cancer cells) and 7.4 (physiological pH). At a 6 h interval, 2 ml of PBS replaced 2 ml of the dialysate, and the quantification of the concentration of the drug released for DOX and TAM was carried out by a UV–visible spectrophotometer using EG.1. at 490 nm and 277 nm, respectively.

$$\text{Drug release } (\%) = \frac{\text{Released drug at a desired time}}{\text{Total amount of drug entrapped within GO} - \text{CS} - \text{FA}} \times 100 \quad (1)$$

Results and discussion

Synthesis, functionalization, and characterization

The modified Hummer's method was employed for synthesizing graphene oxide (GO) nanoparticles in a successful way. The synthesized graphene oxide was sonicated and thus turned into nanographene oxide (GO). Various conjugates were obtained in a successful way with GO viz, graphene oxide chitosan (GO-CS), graphene oxide chitosan folic acid (GO-CS-FA), graphene oxide chitosan folic acid tamoxifen (GO-CS-FA-TAM), and graphene oxide chitosan folic acid tamoxifen doxorubicin (GO-CS-FA-TAM-DOX).

As seen in the samples' UV–vis spectrum (Fig. 1), UV visible spectroscopy provided the distinctive peak of GO at 230 nm, and peaks at 224 nm and 300 nm confirmed that GO was conjugated to chitosan. Peaks at 285 and 366 nm confirmed folic acid conjugation to the chitosan-conjugated GO (GO-CS-FA). The peak seen at

366 nm confirms FA binding because this peak is the characteristic peak of FA [58, 59]. This peak is not seen in GO and GO-CS. The signature absorption peak of the NGO is at 230 nm, which shifted to 285 nm through the formation of an amide bond in FA-NGO (Fig. 1). Furthermore, peaks at 256 nm, 285 nm, and 366 nm (corresponding to TAM) confirmed the loading of TAM to the conjugated GO. The characteristic absorption peak of DOX (~490 nm) [60] appeared in the NGO-CS-FA-TAM-DOX sample, indicating the successful formation of NGO-CS-FA-TAM-DOX conjugates.

It was confirmed by Fourier transform infrared spectroscopy (FTIR) that all samples were conjugated successfully. The recording of the FT-IR spectrum was carried out, and the spectrum of the acquired GO confirmed that graphite was oxidated successfully (Fig. 2). A number of functional groups, e.g., O–H, C–OH, COOH, and C–O, were detected. A broad peak at 3356.31 cm^{-1} in GO's IR spectrum originates from the carboxyl O–H stretching mode. The absorption peaks that correspond to O–H stretching (a peak ~3400 cm^{-1}), superimposed on the OH stretch of carboxylic acid, originate from the existence of absorbed water molecules and alcohol groups [25]. The IR peaks that correspond to 2920.99 cm^{-1} and 2846.83 cm^{-1} originate from the asymmetric and symmetric CH_2 stretching of GO, respectively, whereas the peak around 1620.24 cm^{-1} originates from C=C stretches from the unoxidized graphitic domain. The peak around 1730.06 cm^{-1} originates from the C=O stretch of the carboxyl group [18], the peak at 1219.45 cm^{-1} is due to the C–OH stretch of the alcohol group [27], and peaks at 1357.80 cm^{-1} and 1041.17 cm^{-1} indicate the existence of C–O stretching vibrations of C–O–C.

Chitosan conjugation was confirmed by peaks at 3247.16 (O–H deformation), 1621.54 showing the existence of C=O bonds, 1527.71 corresponding to the bending of N–H in enduring amide groups, 1376.78 and 1054.51 corresponding to C–O bonds [61] (Fig. 2).

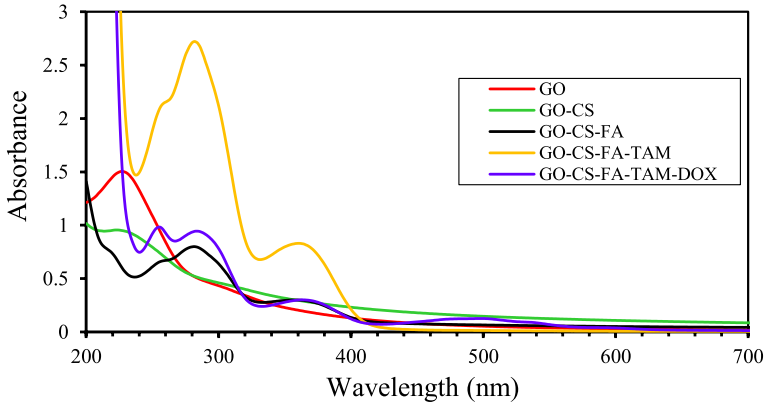

Fig. 1 UV–vis absorbance spectra of GO, GO-CS, GO-CS-FA, GO-CS-FA-TAM and GO-CS-FA-TAM-DOX

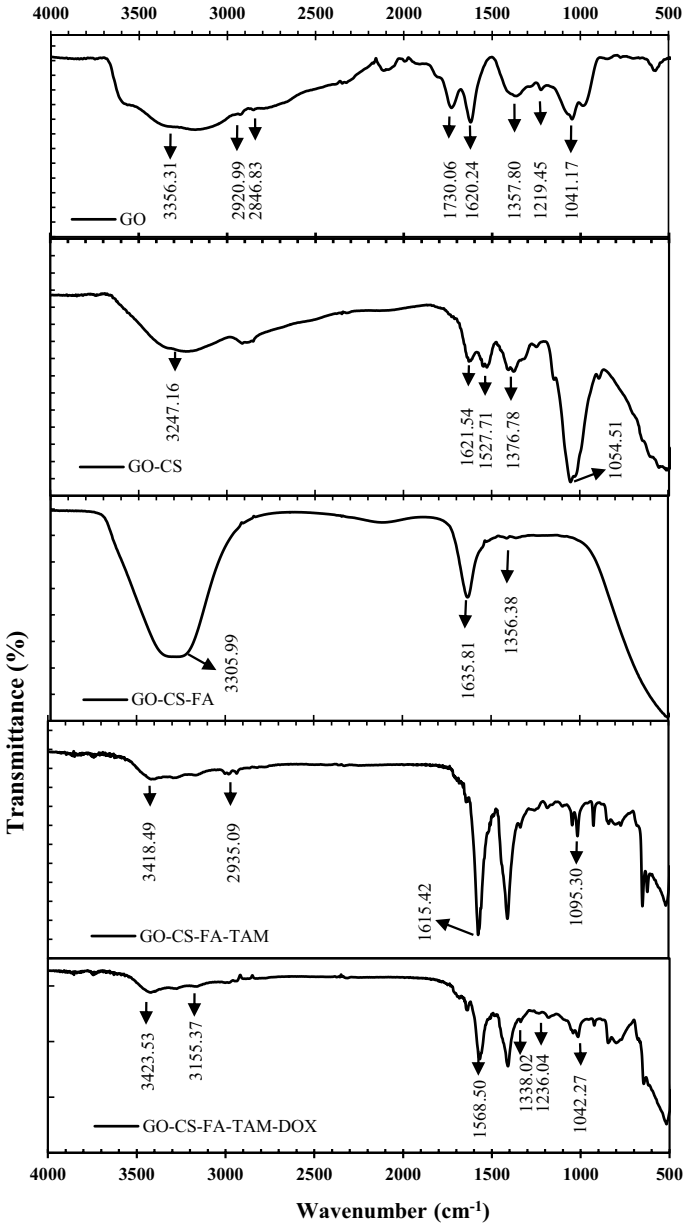

Fig. 2 Fourier transform infrared (FTIR) spectra of GO/GO-CS/GO-CS-FA/GO-CS-FA-TAM/ GO-CS-FA-TAM-DOX

The decoration of folic acid to GO-CS was marked by peaks at 3305.99 (O–H distortion), 1635.81 indicating band superpositions assigned to the amine groups of chitosan and carboxylated groups of GO, and 1356.28 indicating C–O bonds.

With TAM loading, three main characteristic peaks emerged at 3418.47 cm^{-1} (O–H), 1615.42 cm^{-1} (C–O–C), and 1095.30 cm^{-1} (N–H).The peak at 1615.42 cm^{-1} noticed in TAM-loaded samples was determined to be shifted in TAM and DOX-loaded samples with a peak at 1568.50 cm^{-1}.

The FTIR spectrum of GO-CS-FA-TAM-DOX had small shoulders at 3155.37 cm^{-1}, 1338.02 cm^{-1}, 1236.04 cm^{-1}, and 1042.27 cm^{-1}, probably because of the varied quinone and ketone carbonyls of DOX.

The characterization of the synthesized drug-loaded nanobiocomposite was performed by XRD to ensure pure phase identification in Fig. 3. A single peak at 11.8° (JCPDS card number: 75–1621) confirmed GO. Adding folic acid to the chitosan-conjugated GO provided numerous blunt and sharp peaks at 2 theta 18.6°, 29.44°, 34.28°, 40.41° and 45.06°. The combination of TAM and DOX gave prominent peaks at 18.32°, 29.24°, 34.12°, 34.94°, 35.94°, 40.18°, 44.81°, 53.42°, and 58.02°. The XRD data were revealed to be in line with UV visible data, which indicated successful conjugation.

Figure 4 shows SEM images for analyzing the samples' morphological properties in detail. GO sheets were determined to have many wrinkles, while the surface was smoothed and layered following conjugation and drug loading, which indicated correct drug loading (Fig. 4).

Zeta potential is one of the most significant characteristics that can take an essential part in the efficiency of nanomedicine. The stability of targeted therapy or dosage forms can be impacted by the zeta potential of nanomaterials [62]. The nanoparticle surface represents an essential issue in targeting in the drug delivery system. The surface modification of nanocarrier-based systems with hydrophilic polymers is used most frequently for controlling opsonization and improving the system's

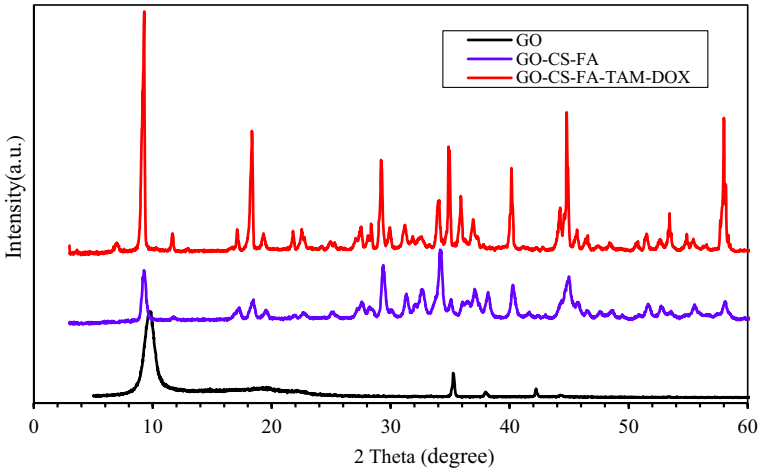

Fig. 3 Showing XRD pattern of GO, GO-CS-FA and GO-CS-FA-TAM-DOX

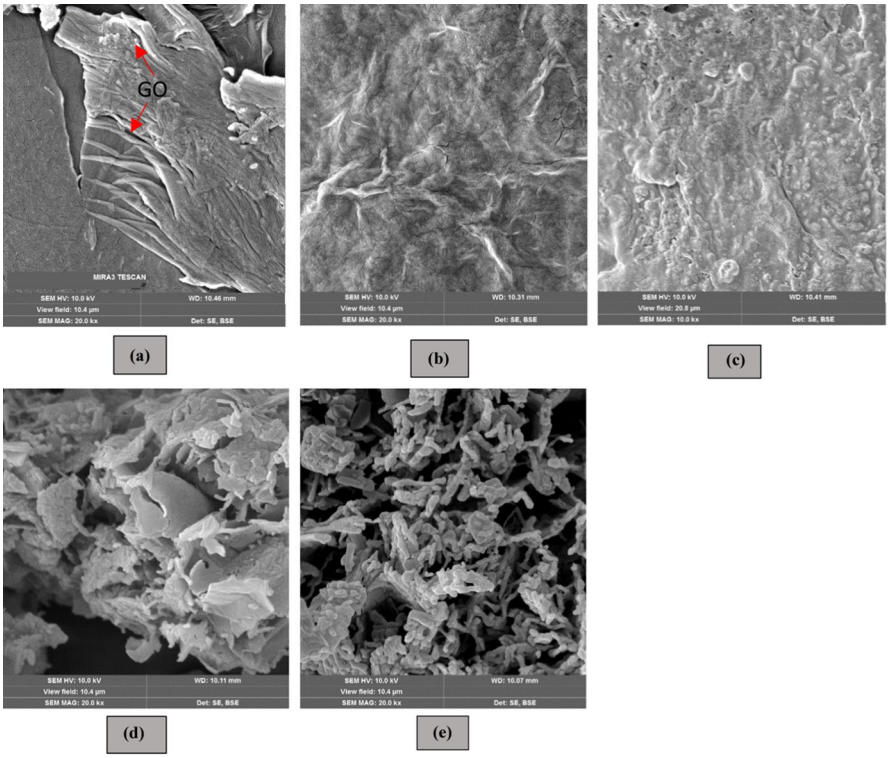

Fig. 4 SEM images showing **a** GO **b** GO-CS **c** GO-CS-FA **d** GO-CS-FA-TAM and **e** GO-CS-FA-TAM-DOX

surface features, particularly the surface charge. In the present study, surface modification was performed using chitosan in the drug delivery system, and an important feature in targeting was researched by examining the samples' zeta potential. The tumor takes up positively charged nanoparticles preferentially and retains them for a longer duration than negatively charged or neutral particles since phosphatidyl serine, which is a negatively charged residue, is translocated to cancer cells' surface and tumor cells can translocate positively charged nanoparticles via either fluid-phase endocytosis, or charge interactions and ligand-receptor docking [63–66]. As a result of the zeta potential analysis, while GO had a negative zeta potential value, it became positively charged by decorating the surface with CS (Fig. 5). Negative surface charge is anticipated to induce electrostatic repulsion, which in turn, confers physical stability of GO via preventing the formation of aggregates. The zeta potential value of GO-CS-FA was relatively higher than that of GO-CS. For all samples, zeta potential values greater than ± 25 mV show a high stability of drug delivery systems because of the efficient electrostatic particle repulsion.

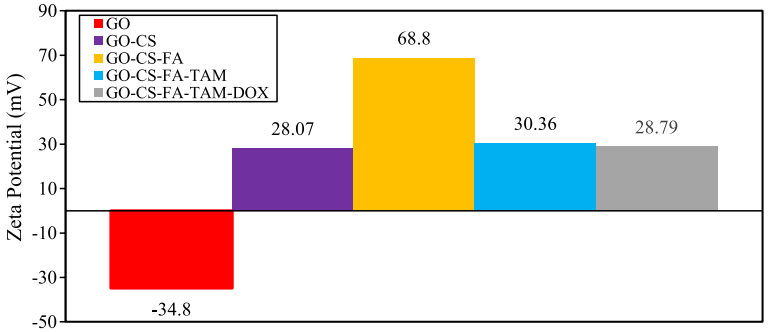

Fig. 5 Zeta potential of **a** GO **b** GO-CS **c** GO-CS-FA **d** GO-CS-FA-TAM and **e** GO-CS-FA-TAM-DOX at room temperature

Drug loading and release

In line with the literature, it is possible to attribute the loading of TAM and DOX onto GO-CS-FA to non-covalent interactions, π–π stacking and strong electrostatic interactions occurred between the cationic CS and the negatively charged GO. Non-covalent method is based on the electrostatic interaction and van der Waals forces [67]. This process does not change the chemical structure, and it is easy to perform. The main intermolecular interactions observed in the noncovalent modification of graphene are π–π interactions and hydrogen bonding. A peak acquired at 277 nm and the increased intensity of a peak at 490 nm that corresponds to the DOX peak of GO-CS-FA-TAM-DOX in the UV visible spectra analysis can confirm the loading of TAM onto GO-CS-FA (Fig. 1). Furthermore, the loading efficiency was computed as 45%.

The TAM and DOX release behavior was researched in phosphate buffer saline (PBS) at two pH values (5.8 and 7.4). The total amount of TAM and DOX released from the drug delivery system (GO-CS-FA-TAM-DOX) over 24 h was nearly 22% and 20% for TAM and 30% and 25% for DOX at pH 5.8 and pH 7.4, respectively. The drug release rate from the drug delivery system at pH 5.8, regarded as the endosomal pH of cancer cells, was more rapid than that at pH 7.4 (Figs. 6 and 7) [68]. The said quicker release at a lower pH value (PBS, pH 5.8) was attributed to higher solubility at acidic pH and thus ensuring that drugs leached out at a considerably higher rate. Additionally, it is seen that DOX has a higher release rate than TAM at both pH values. Hence, it could be expected that the drugs would ensure a pH-responsive release profile for entrapped drugs in vivo. The mentioned pH-dependent drug release behavior is essential in clinical applications due to the acidic character of microenvironments in intracellular lysosomes and endosomes and extracellular tumor tissues.

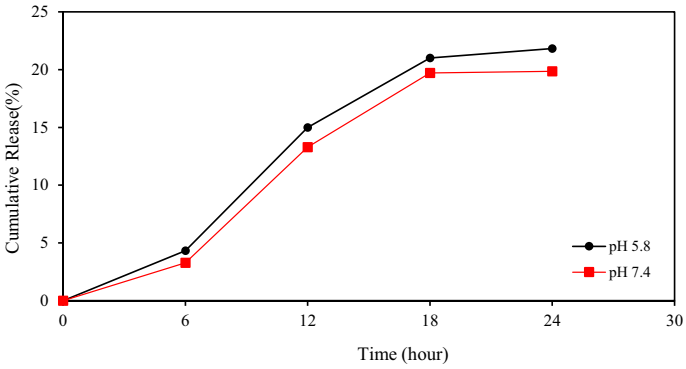

Fig. 6 In vitro drug release (TAM) profile from GO-CS-FA-TAM-DOX at pH 5.8 and pH 7.4

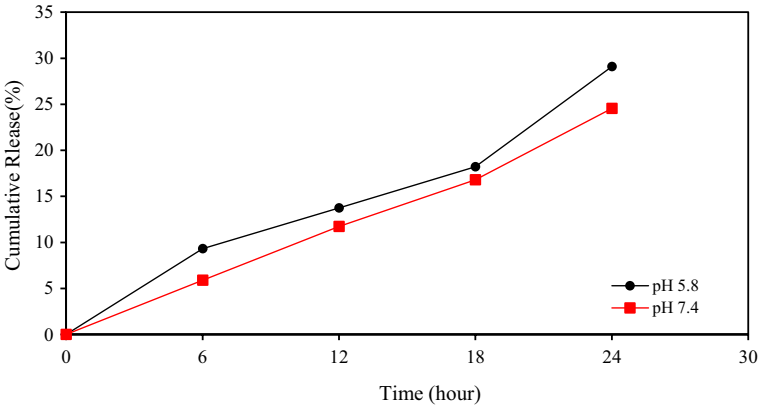

Fig. 7 In vitro drug release (DOX) profile from GO-CS-FA-TAM-DOX at pH 5.8 and pH 7.4

Conclusions

To sum up, we described the synthesis of an effective drug delivery system, GO-CS-FA, loaded with anticancer drugs, and tested drug loading and in vitro controlled release. First, the synthesis of GO nanoparticles and their conjugation with CS were performed with the objective of enhancing the drug's biocompatibility and providing it with solubility. For specific targeting of the cancer cells, the conjugation of GO-CS with folic acid was carried out. There is an excessive affinity of folic acid for the internal folate receptor, and, thus, it is researched for targeting numerous cancer types, which are folate receptors. Then TAM and DOX were loaded onto the GO-CS-FA drug delivery system. A high drug loading capacity and pH-dependent drug release were confirmed. The total amount of TAM and DOX released from the drug delivery system (GO-CS-FA-TAM-DOX) over 24 h was nearly 22% and 20% for TAM and 30% and 25% for DOX at pH 5.8 and pH 7.4, respectively. Hence, this study demonstrates that it is feasible to use

functionalized GO as a possible drug delivery agent in cancer therapy. In general, the combinatorial impact generated by the TAM-DOX-loaded nanobiocomposite may act as a chemotherapeutic agent with high potential against breast cancer with enhanced bioavailability and fewer side impacts since it is targeted. There is a need for more studies to show the effectiveness of drug delivery by the nanocarrier under in vitro and in vivo conditions.

References

1. van der Zee J (2002) Heating the patient: a promising approach? Ann Oncol 13(8):1173–1184
2. Siegel RL, Miller KD, Jemal A (2019) Cancer statistics, 2019. CA Cancer J Clin 69(1):7–34
3. Thomadaki H, Scorilas A (2008) Molecular profile of breast versus ovarian cancer cells in response to treatment with the anticancer drugs cisplatin, carboplatin, doxorubicin, etoposide and taxol. Biol Chem 389(11):1427–1434
4. Bronchud MH, Howell A, Crowther D, Hopwood P, Souza L, Dexter TM (1989) The use of granulocyte colony-stimulating factor to increase the intensity of treatment with doxorubicin in patients with advanced breast and ovarian cancer. Br J Cancer 60(1):121–125
5. Ikeda M et al (2011) The radiotherapy with methotrexate, vinblastine, doxorubicin, and cisplatin treatment is an effective therapeutic optionin patients with advanced or metastatic bladder cancer. J Radiat Res 52(5):674–679
6. Huober J, Schoch O, Templeton A, Spirig C, Thürlimann B (2010) Interstitial pneumonitis after treatment with bevacizumab and pegylated liposomal doxorubicin in a patient with metastatic breast cancer. Chemotherapy 56(1):69–70
7. Minotti G, Menna P, Salvatorelli E, Cairo G, Gianni L (2004) Anthracyclines: molecular advances and pharmacologie developments in antitumor activity and cardiotoxicity. Pharmacol Rev 56(2):185–229
8. Kim D, Lee ES, Oh KT, Gao Z, Bae YH (2008) Doxorubicin-loaded polymeric micelle overcomes multidrug resistance of cancer by double-targeting folate receptor and early endosomal pH. Small 4(11):2043–2050
9. Betancourt T, Brown B, Brannon-Peppas L (2007) Doxorubicin-loaded PLGA nanoparticles by nanoprecipitation: preparation, characterization and in vitro evaluation. Nanomedicine 2(2):219–232
10. Chang M (2012) Tamoxifen resistance in breast cancer. Biomol Ther 20(3):256–267
11. Zhang L, Lu J, Jin Y, Qiu L (2014) Folate-conjugated beta-cyclodextrin-based polymeric micelles with enhanced doxorubicin antitumor efficacy. Colloids Surf B Biointerfaces 122:260–269
12. Patel HK, Bihani T (2018) Selective estrogen receptor modulators (SERMs) and selective estrogen receptor degraders (SERDs) in cancer treatment. Pharmacol Ther 186:1–24
13. How CW, Rasedee A, Manickam S, Rosli R (2013) Tamoxifen-loaded nanostructured lipid carrier as a drug delivery system: characterization, stability assessment and cytotoxicity. Colloids Surf B Biointerfaces 112:393–399
14. Hertl M, Cosimi AB (2005) Liver transplantation for malignancy. Oncologist 10(4):269–281
15. Lazzeroni M, Serrano D, Dunn BK, Heckman-Stoddard BM, Lee O, Khan S, Decensi A (2012) Oral low dose and topical tamoxifen for breast cancer prevention: modern approaches for an old drug. Breast Cancer Res 14(5):1–11
16. Vivek R, Nipun Babu V, Thangam R, Subramanian KS, Kannan S (2013) pH-responsive drug delivery of chitosan nanoparticles as Tamoxifen carriers for effective anti-tumor activity in breast cancer cells. Colloids Surf B Biointerfaces 111:117–123
17. Chuang P-Y, Huang C, Huang H-C (2013) The use of a combination of tamoxifen and doxorubicin synergistically to induce cell cycle arrest in BT483 cells by down-regulating CDK1, CDK2 and cyclin D expression. J Pharm Technol Drug Res 2(1):12
18. Youlden DR, Cramb SM, Dunn NAM, Muller JM, Pyke CM, Baade PD (2012) The descriptive epidemiology of female breast cancer: an international comparison of screening, incidence, survival and mortality. Cancer Epidemiol 36(3):237–248
19. Kateb B et al (2011) Nanoplatforms for constructing new approaches to cancer treatment, imaging, and drug delivery: what should be the policy? Neuroimage 54(SUPPL.1):1

20. He Z, Zhang Z, Bi S (2020) Nanoparticles for organic electronics applications. Mater Res Express 7(1):012004
21. Sousa De Almeida M, Susnik E, Drasler B, Taladriz-Blanco P, Petri-Fink A, Rothen-Rutishauser B (2021) Understanding nanoparticle endocytosis to improve targeting strategies in nanomedicine. Chem Soc Rev 50(9):5397–5434
22. Kazempour M, Namazi H, Akbarzadeh A, Kabiri R (2019) Synthesis and characterization of PEG-functionalized graphene oxide as an effective pH-sensitive drug carrier. Artif Cells Nanomed Biotechnol 47(1):90–94
23. Gao X, Li L, Cai X, Huang Q, Xiao J, Cheng Y (2021) Targeting nanoparticles for diagnosis and therapy of bone tumors: opportunities and challenges. Biomaterials 265:120404
24. Goenka S, Sant V, Sant S (2014) Graphene-based nanomaterials for drug delivery and tissue engineering. J Control Release 173(1):75–88
25. Swain AK, Pradhan L, Bahadur D (2015) Polymer stabilized Fe_3O_4-graphene as an amphiphilic drug carrier for thermo-chemotherapy of cancer. ACS Appl Mater Interfaces 7(15):8013–8022
26. Zare EN, Makvandi P, Ashtari B, Rossi F, Motahari A, Perale G (2020) Progress in conductive polyaniline-based nanocomposites for biomedical applications: a review. J Med Chem 63(1):1–22
27. Ulery BD, Nair LS, Laurencin CT (2011) Biomedical applications of biodegradable polymers. J Polym Sci Part B Polym Phys 49(12):832–864
28. Peer D, Karp JM, Hong S, Farokhzad OC, Margalit R, Langer R (2007) Nanocarriers as an emerging platform for cancer therapy. Nat Nanotechnol 2(12):751–760
29. Wu J (2021) The enhanced permeability and retention (EPR) effect: the significance of the concept and methods to enhance its application. J Pers Med 11(8):771
30. Byrne JD, Betancourt T, Brannon-Peppas L (2008) Active targeting schemes for nanoparticle systems in cancer therapeutics. Adv Drug Deliv Rev 60(15):1615–1626
31. Varshosaz J, Hassanzadeh F, Sadeghi H, Khadem M (2012) Galactosylated nanostructured lipid carriers for delivery of 5-FU to hepatocellular carcinoma. J Liposome Res 22(3):224–236
32. Chen YW, Su YL, Hu SH, Chen SY (2016) Functionalized graphene nanocomposites for enhancing photothermal therapy in tumor treatment. Adv Drug Deliv Rev 105:190–204
33. Gazzi A et al (2019) Photodynamic therapy based on graphene and MXene in cancer theranostics. Front Bioeng Biotechnol 7:295
34. Pei X, et al. PEGylated nano-graphene oxide as a nanocarrier for delivering mixed anticancer drugs to improve anticancer activity, nature.com
35. Veclani D, Tolazzi M, Melchior A (2020) Molecular interpretation of pharmaceuticals' adsorption on carbon nanomaterials: theory meets experiments. Processes 8(6):642
36. Aliyev E, Filiz V, Khan MM, Lee YJ, Abetz C, Abetz V (2019) Structural Characterization of graphene oxide: surface functional groups and fractionated oxidative debris. Nanomater 9(8):1180
37. Eckhart KE, Holt BD, Laurencin MG, Sydlik SA (2019) Covalent conjugation of bioactive peptides to graphene oxide for biomedical applications. Biomater Sci 7(9):3876–3885
38. Tabish TA et al (2019) Graphene oxide-based targeting of extracellular cathepsin D and Cathepsin L as a novel anti-metastatic enzyme cancer therapy. Cancers (Basel) 11(3):319
39. Gu Z, Zhu S, Yan L, Zhao F, Zhao Y (2019) Graphene-based smart platforms for combined cancer therapy. Adv Mater 31(9):1800662
40. Tadyszak K, Wychowaniec JK, Litowczenko J Biomedical applications of graphene-based structures
41. Tas A, Keklikcioglu Cakmak N (2021) Synthesis of PEGylated nanographene oxide as a nanocarrier for docetaxel drugs and anticancer activity on prostate cancer cell lines. Hum Exp Toxicol 40(1):172–182
42. Deb A, Andrews NG, Raghavan V (2018) Natural polymer functionalized graphene oxide for co-delivery of anticancer drugs: in-vitro and in-vivo. Int J Biol Macromol 113:515–525
43. Feng W, Wang Z Biomedical applications of chitosan-graphene oxide nanocomposites
44. Pooresmaeil M, Namazi H (2022) "Chitosan based nanocomposites for drug delivery application. Nanotechnology for biomedical applications. Springer, Singapore, pp 135–201
45. Khan NK, Azad TA, Fuloria AK, Nawaz S, Subramaniyan A, Akhlaq V et al (2021) Chitosan-coated 5-fluorouracil incorporated emulsions as transdermal drug delivery matrices. Polym (Basel) 13(19):33
46. Pooresmaeil M, Namazi H (2020) Facile preparation of pH-sensitive chitosan microspheres for delivery of curcumin; characterization, drug release kinetics and evaluation of anticancer activity. Int J Biol Macromol 162:501–511

47. Farhoudian S, Yadollahi M, Namazi H (2016) Facile synthesis of antibacterial chitosan/CuO bionanocomposite hydrogel beads. Int J Biol Macromol 82:837–843
48. Keklikcioğlu Çakmak N, Küçükyazıcı M, Eroğlu A (2019) Synthesis and stability analysis of folic acid-graphene oxide nanoparticles for drug delivery and targeted cancer therapies. Int Adv Res Eng J 03(02):81–85
49. Schnoell J, Jank BJ, Kadletz-Wanke L, Stoiber S, Gurnhofer E, Schlederer M, Heiduschka G, Kenner L (2022) Protein expression of folate receptor alpha in adenoid cystic carcinoma of the head and neck. OncoTargets Ther 15:531
50. Sun C, Sze R, Zhang M (2006) Folic acid-PEG conjugated superparamagnetic nanoparticles for targeted cellular uptake and detection by MRI. J Biomed Mater Res Part A 78(3):550–557
51. Oh JK, Park JM (2011) Iron oxide-based superparamagnetic polymeric nanomaterials: design, preparation, and biomedical application. Prog Polym Sci (Oxford) 36(1):168–189
52. Deb A, Vimala R (2018) Camptothecin loaded graphene oxide nanoparticle functionalized with polyethylene glycol and folic acid for anticancer drug delivery. J Drug Deliv Sci Technol 43(November):333–342
53. Qin XC, Guo ZY, Liu ZM, Zhang W, Wan MM, Yang BW (2013) Folic acid-conjugated graphene oxide for cancer targeted chemo-photothermal therapy. J Photochem Photobiol B Biol 120:156–162
54. Low PS, Henne WA, Doorneweerd DD (2008) Discovery and development of folic-acid-based receptor targeting for imaging and therapy of cancer and inflammatory diseases. Acc Chem Res 41(1):120–129
55. Marcano DC et al (2010) Improved synthesis of graphene oxide. ACS Nano 4(8):4806–4814
56. P Ghasemiyeh, S Mohammadi-Samani, Polymers blending as release modulating tool in drug delivery
57. Arkaban H et al (2022) Polyacrylic acid nanoplatforms: antimicrobial, tissue engineering, and cancer theranostic applications. Polymers 14:1259
58. Jain S, Rathi VV, Jain AK, Das M, Godugu C (2012) Folate-decorated PLGA nanoparticles as a rationally designed vehicle for the oral delivery of insulin. Nanomedicine 7(9):1311–1337
59. Mortazavi N, Heidari M, Rabiei Z, Enferadi ST, Monazzah M (2021) Loading harmine on nanographene changes the inhibitory effects of free harmine against MCF-7 and fibroblast cells. Med Chem Res 30(5):1108–1116
60. Xie BX et al (2022) Folic acid-modified metal-organic framework carries CPT and DOX for cancer treatment. J Solid State Chem 306:122803
61. Hosseini SM et al (2022) Designing chitosan nanoparticles embedded into graphene oxide as a drug delivery system. Polym Bull 79(1):541–554
62. Lee H et al (2022) Hypoxia-responsive nanomedicine to overcome tumor microenvironment-mediated resistance to chemo-photodynamic therapy. Mater Today Adv 14:100218
63. Cafaggi S et al (2007) Preparation and evaluation of nanoparticles made of chitosan or N-trimethyl chitosan and a cisplatin-alginate complex. J Control Release 121(1–2):110–123
64. Park JH, Saravanakumar G, Kim K, Kwon IC (2010) Targeted delivery of low molecular drugs using chitosan and its derivatives. Adv Drug Deliv Rev 62(1):28–41
65. Chun CJ, Lee SM, Kim SY, Yang HK, Song SC (2009) Thermosensitive poly(organophosphazene)-paclitaxel conjugate gels for antitumor applications. Biomaterials 30(12):2349–2360
66. Honary S, Zahir F (2013) Effect of zeta potential on the properties of nano-drug delivery systems - a review (part 1). Trop J Pharm Res 12(2):255–264
67. TM Magne, et al. (2021) Graphene and its derivatives: understanding the main chemical and medicinal chemistry roles for biomedical applications, no. 0123456789. Springer Berlin Heidelberg
68. De Sousa M, De Luna LAV, Fonseca LC, Giorgio S, Alves OL (2018) Folic-acid-functionalized graphene oxide nanocarrier: synthetic approaches, characterization, drug delivery study, and antitumor screening. ACS Appl Nano Mater 1:922–932